in the range of 100–1000 nm, have been frequently exploited as carriers for macromolecules [e.g., plasmid DNA, siRNA, peptides, and genes] and small molecules [e.g., a corticosteroid and alkaloids]. The details of these applications have been described in a recent review by Taira et al. (2009). NPs have also found practical application in mass spectrometry (MS) research.

Historically, one of the currently employed *"standard"* soft ionization techniques in MS, matrix-assisted laser desorption/ionization (MALDI), was initiated by Tanaka's study, which was awarded the Nobel Prize in Chemistry; in this technique, a suspension of an inorganic NP such as cobalt, silicon, or titanium nitride was utilized as an analyte ionization enhancing reagent, referred to as a matrix (Tanaka et al. 1988). Although subsequent studies have successively developed various series of organic matrix compounds, which are currently the most frequently used matrices (Karas and Hillenkamp 1988), NPs have again begun to attract increasing attention owing to the progress in technology, which has resulted in the production of a wide variety of NPs. The increasing availability of various kinds of NPs, especially with variations in sizes, core materials, and surface coating/chemical modifications, has allowed researchers the option of choice from a selection of NPs to suit the chemical/physical requirements of their research purposes. In fact, the use of NPs as an alternative to organic matrices in MS research has been widely studied, particularly in the analyses of small molecules. In this regard, the use of NPs offers a number of attractive advantages including the elimination of noise generated by the organic matrix compounds. In addition, based on the proper choice of core metal material and surface modification, analyte molecules that are difficult to ionize using conventional organic matrices can be very efficiently ionized using NP matrices (Su and Tseng 2007).

This chapter describes the application of NPs to the emerging MS methodology known as imaging mass spectrometry (IMS). In IMS, which is an MS based molecular imaging technique, distributions of analyte molecules are visualized from the mass spectra obtained from thousands of data points collected from thin biological tissue sections as well as inorganic samples. Owing to the MS-based detection principle, IMS has now opened up a new frontier, particularly in the imaging of a variety of small organic molecules, such as endogenous metabolites, and the *in vivo* monitoring of administered drugs (within the animal/human body). The most frequently used ionization techniques are MALDI or SIMS (secondary ion mass spectrometry) (Yang et al. 2010) and recently, the application of NP-assisted laser desorption/ionization (nano-PALDI) has been initiated.

IMAGING MASS SPECTROMETRY (IMS)

Principles of MS and IMS

MS is an analytical technique that measures the mass-to-charge (m/z) ratio of charged atoms, molecules, and molecular clusters/fragments. MS is one of the fastest and most reliable methods for the high-accuracy determination of the mass of analyte particles. A typical mass spectrometer is composed of several functionally distinct components—an ion source, a mass analyzer, and a detector. Within the ion source, the analyte atoms or molecules are ionized by means of various ionization techniques; the analyzer then separates the ions on the basis of their m/z values and the detector outputs electrical signals in response to the reception of separated ions. The mass spectra can then be constructed from these signals (Fig. 1). The development of analyte ionization techniques, including recent progress in the soft-ionization technique, particularly MALDI and electrospray ionization (ESI), has opened up the possibility for the analysis of quite a wide range of molecules using a simple procedure, especially for large biopolymers such as proteins, nucleotides, and polysaccharides. MALDI, in particular, permits the analysis of solid phase samples and has therefore has been adopted in IMS from early studies mainly for biological tissue samples (Stoeckli et al. 2001). The details of this application are further discussed in a subsequent section. The MALDI process is triggered by a laser beam. An organic matrix compound is used to protect the large

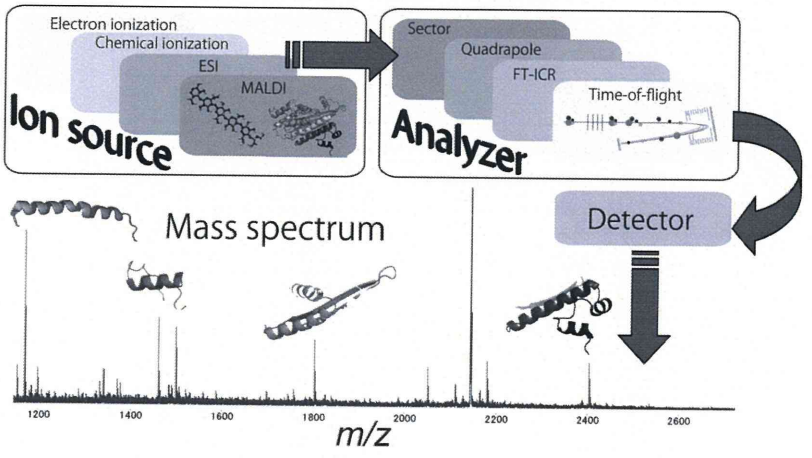

Fig. 1. Principle schematic of mass spectrometer. A typical mass spectrometer consists of three separate components—an ion source, a mass analyzer, and a detector. Numerous variations have been developed for each component based on different principles.

biomolecules from being destroyed by direct contact with the laser beam and to facilitate vaporization and ionization. The currently derived, general versatility of MALDI was established by a momentous effort directed at the development of novel matrix compounds suitable for the ionization of various molecules of interest. This effort has, therefore, facilitated the utilization of MALDI-IMS for the visualization of a variety of molecules (Sugiura and Setou 2010a).

Figure 2 illustrates the general workflow of MALDI-IMS. The basic technique involves the mounting of thin tissue slices on conductive glass slides and application of a suitable MALDI matrix to the tissue section. The slide is then inserted into a mass spectrometer and a focused laser beam is directed at predetermined positions of the tissue slice. The mass spectrometer records the spatial distribution of the molecular species (typically with a 10–200 μm scan pitch). Automated data collection takes 2–6 h, depending on the number of points assayed. Appropriate image processing software is required to import data from the mass spectrometer in order to allow visualization of the ion distribution images and comparison with the histological images of the sample. The unique advantages of MALDI imaging that facilitate the versatility of IMS as a molecular imaging technique are summarized as follows. (1) IMS does not

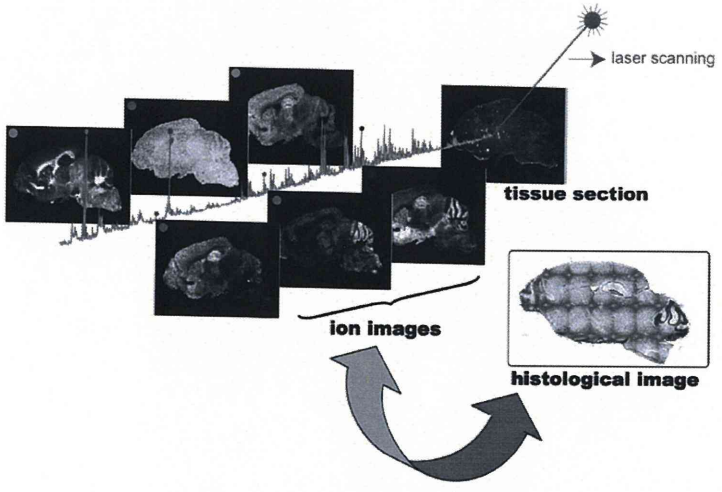

Fig. 2. Schematic representation of matrix-assisted laser desorption/ionization imaging mass spectrometry (MALDI-IMS) procedures. The MALDI laser scans through a set of preselected locations on the tissue (10–200 μm scan pitch), and the mass spectrometer records the spatial distribution of molecular species. Suitable image processing software can be used to import data from the mass spectrometer to allow visualization and comparison with the histological image of the sample.

require any specific chemical labels or probes. (2) IMS is a "non-targeted" imaging method. (3) The simultaneous imaging of multiple types of molecular species is possible. With the unique and powerful detection principle facilitated by MS, the MALDI-imaging mass spectrometry (IMS) can be used for the visualization of the distribution of a large number of biomolecules in cells and tissues, ranging from small metabolite molecules (Khatib-Shahidi et al. 2006) to much larger proteins (Chaurand et al. 2006).

IMS Applications to Areas of Health and Diseases

Current MALDI-IMS applications can be subdivided into two major categories, namely, IMS analysis of large proteins/peptides and IMS analysis of small organic molecules. In the early days, most of the reports on MALDI-IMS were geared at the detection and imaging of proteins or peptides. This area of application particularly targeted the detection of biomarker proteins, which localize specifically in lesions, by utilizing the capacity of IMS for the direct and simultaneous detection of multiple proteins in the tissues. Figure 3a shows one of the earliest medical application studies, which reports the detection and imaging of cancer-specific proteins in a mouse glioma model (Chaurand et al. 2004). As discussed previously, one of the significant advantages of IMS is that a number of cancer/normal specific protein distribution images can be acquired in a non-targeted manner from a single measurement. In addition, disease diagnosis by distinguishing between normal and cancerous biopsy specimens has been attempted by statistical evaluation of such multiple protein expression levels. Figure 3b shows that by applying hierarchical clustering analyses of IMS datasets obtained from human lung specimens, Yanagisawa et al. (2003) achieved successful classification of not only normal and cancerous biopsy samples but also of different cancer types, i.e., primary and non-primary non-small cell lung cancer. Such IMS-based molecular diagnosis studies continue to attract growing attention.

Another major medical application of IMS to the analysis of small molecules is conducted in the pharmaceutical field, e.g., for pharmacokinetic monitoring, pharmacotoxicology, and pharmacometabolomics (Fig. 4). For example, an important phase of drug discovery is determining how a drug-candidate compound is distributed and metabolized within the body. The application of IMS to the monitoring of drug delivery has also attracted much interest. Compared to traditional whole-body autoradiography (WBA) using radio labeled compounds, IMS offers many advantages in the determination of drug distribution. First, IMS allows for the simultaneous and discriminate monitoring not only of the intact drug molecules, but also of their metabolites (Khatib-Shahidi et al. 2006), whereas WBA cannot

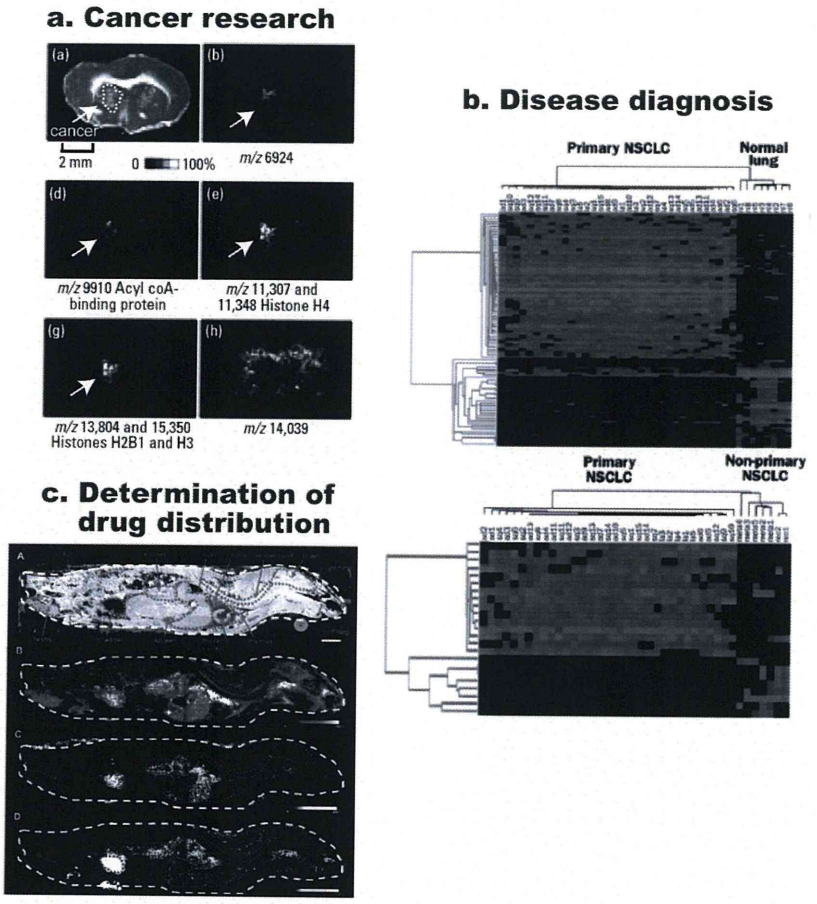

Fig. 3. Representative imaging mass spectrometry (IMS) applications in areas of health and diseases. Shown are representative examples of IMS application to brain cancer research using the mouse glioma model (a); human disease diagnosis of healthy and different types of lung cancers (b); and determination of pharmacokinetics in the whole animal body (c). NSCLC = non-small cell lung cancer. Reprinted from Chaurand et al. 2004 (a); Yanagisawa et al. 2003 (b); and Khatib-Shahidi et al. 2006 (c) with permission of ACS Publications (a and b) and Elsevier, Ltd. (c).

distinguish these molecules. Thus, IMS can be used to determine whether or not medicinally intact drugs have reached the target organs. Secondly, IMS can be used to visualize the distribution of drugs at a lower cost and in a much shorter time than with detection using isotopes. Figure 3c shows the detection of drugs that have been delivered orally to mice. In this study, the distribution of the antipsychotic drug olanzapine and its metabolites in

the sagittal section of an intact (whole) rat was successfully investigated 6 h after administration. This study clearly showed the distinct distribution of intact drugs and their metabolites; the intact drug reached the target organ (the brain), whereas its metabolites were localized in the bladder.

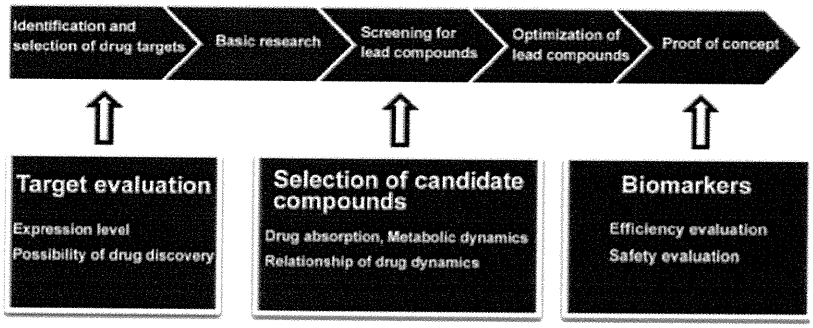

Fig. 4. Processes of new drug development and areas of application of imaging mass spectrometry (IMS) in each step. New drug development can be divided into several processes. IMS can be widely applied to many of the steps along the way through the ability to visualize various molecules.

APPLICATION OF NANOPARTICLES TO IMS

Utilization of a Variety of NPs in Basic MS Research

As described previously, MALDI had its genesis as a soft-ionization technique employing NPs (Tanaka et al. 1988). Since then, rapid technical progress over the ensuing couple of decades has made NP handling much easier, and studies on the utilization of NPs as ionization assisting reagents have been intensively reported. The main motivation behind the use of NP-assisted ionization is to overcome the limitations of MALDI, particularly for the detection of molecules in the low mass range, without interference from matrix-derived ions. The low m/z region of a MALDI spectrum contains a large population of ions from biological metabolites as well as matrix-related adduct clusters and fragments, which are dominantly observed in the MALDI mass spectrum. This high density of ions increases the risk of sharing of the same mass window by matrix ions and analyte molecules. The utilization of NPs as a matrix is one of the effective methods for prevention of this problem, because the NPs produce few background ions. Figure 5 shows an example in which reserpine, an indole alkaloid antipsychotic and antihypertensive drug, was analyzed using both fNP and α-cyano-4-hydroxycinnamic acid (CHCA) as respective matrices. The spectra presented clearly demonstrate the complete elimination of background ions by use of NPs (Sahashi et al. 2010). Furthermore, the

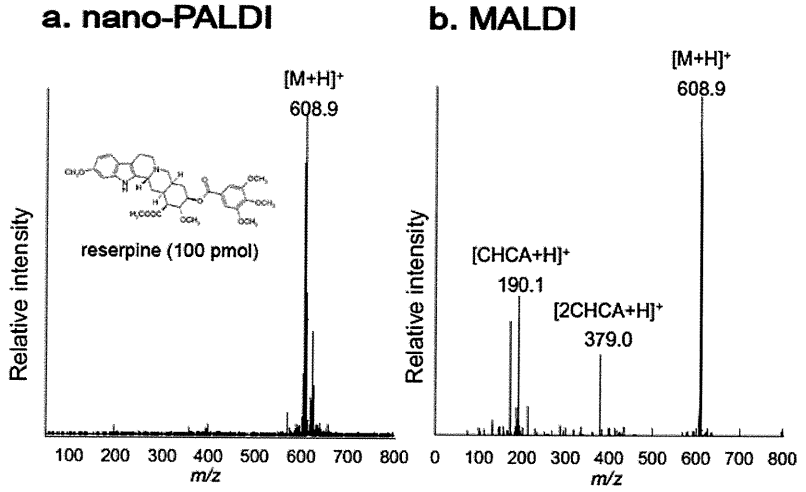

Fig. 5. Comparison between mass spectra obtained by nanoparticle-assisted laser desorption/ionization (nano-PALDI) and matrix-assisted laser desorption/ionization (MALDI). Mass spectra of reserpine, an indole alkaloid antipsychotic and antihypertensive drug, obtained by both nano-PALDI and MALDI-mass spectrometry in which functional nanoparticle (fNP) and α-cyano-4-hydroxycinnamic acid (CHCA) were used as matrices, respectively. This example clearly demonstrates the complete elimination of background ions by use of NPs. Reprinted from Sahashi et al. 2010 with the permission of Elsevier, Ltd.

use of NPs has improved the homogeneity of analyte distribution in the samples on the target plate, which could increase sample-to-sample reproducibility. In comparison, the crystallization process in MALDI inevitably causes artificial localization of analyte molecules within the sample; therefore, researchers have had to locate a *hot spot* where the analytes were concentrated by moving the laser irradiation spots. This is a time-consuming process and one of the major reasons for the lowered quantitative performance of MALDI.

In addition to these general advantages of NP-assisted ionization, a variety of characteristic NPs have been used for analyte-specific MS research (as summarized in Table 1). For example, graphite NPs have been utilized for the detection of relatively large molecules such as peptides and proteins from liquid solutions, with sensitivities in the pico- to nanomole range (Sunner et al. 1995). Bifunctional magnetic iron oxide particles immobilized on silane have also been used for the analysis of proteins and peptides (Chen and Chen 2006). Recently, citrate capped gold nanoparticles (AuNPs) have been utilized for the analyses of important signaling biomolecules—progesterone, testosterone, and cortisol (Wu et al. 2009), which are difficult to detect using conventional organic matrices. Silver

Table 1. Representative nanoparticle assisted laser desorption/ionization technique and its applications. Listed are representative mass spectrometry studies in which various nanoparticles were utilized as ionization enhancing reagents; applied to the measurement of biological molecules.

Name of NP	Core metal	Diameter	Analyte	Reference	Imaging
AgNPs	Ag	3.84±0.45nm	Fatty acids	Hayasaka et al. 2010	yes
		34±3nm	Estrogen	Chiu et al. 2008	yes
					yes
MnNPs	MnO_2, $Mn2O_3$	5.4±0.2nm	Ginsenosides	Sahashi et al. 2010	yes
fNP	Fe_2O_3	3.7nm	Phospholipids	Moritake et al. 2009	yes
			Sulfatide	Ageta et al. 2009	yes
			Lipids, peptides	Taira et al. 2008	yes
AuNPs	Au	4.3±0.7nm	Glycosphingolipids	Goto-Inoue et al. 2010	yes
		13.2±1.2nm	Progesterone, Cortisol, Testesteron	Wu et al. 2009	no
TiO_2 NPs	TiO_2	<0.05μm	Trypsinogen	Watanabe et al. 2009	no

Ageta et al. 2009. Med. Mol. Morphol. 42: 16–23.
Chiu et al. 2008. J. Am. Soc. Mass. Spectrom. 19: 1343–1346.
Goto-Inoue et al. 2010. J. Am. Soc. Mass. Spectrom. 21: 1940–1943.
Hayasaka et al. 2010. J. Am. Soc. Mass. Spectrom. 21: 1446–1454.
Moritake et al. 2009. J. Nanosci. Nanotechnol. 9: 169–176.
Sahashi et al. 2010. Food Chem. 123: 865–871.
Taira, S. et al. 2008. Anal. Chem. 80: 4761–4766.
Watanabe et al. 2009. J. Mass Spectrom. 44: 1443–1451.
Wu et al. 2009. J. Am. Soc. Mass. Spectrom. 20: 875–882.

nanoparticles (AgNPs) capped with several types of functional groups have been used for the detection of sulfur drugs and biothiols (Shrivas and Wu 2008). It has also been demonstrated that AgNPs can selectively ionize cholesterol, phosphatidylcholine, and carotenoids (Sherrod et al. 2008). Moreover, AgNPs have also been used for the determination of small molecular hormones, such as estrone, estradiol, and estriol (Chiu et al. 2008). In another study, titanium dioxide (TiO_2) NPs modified with urea have been shown to increase the ionization efficiency of analytes owing to the photocatalytic effect of TiO_2, which was easily activated by UV irradiation. Furthermore, the modified TiO_2 NPs could also be applied to the detection of large proteins of sizes greater than 20 kDa, such as trypsinogen (Watanabe et al. 2009).

Nano-PALDI for IMS

The usefulness of MALDI-based IMS was briefly reviewed in the preceding sections; however, utilization of the NP-assisted ionization technique is an attractive alternative to MALDI. In this context, utilization of NPs in IMS is expected to be a quite useful tool, especially for the imaging of small molecule distribution, and therefore, this state-of-the-art imaging technology, nano-PALDI-based IMS, and its future perspectives are discussed in the following sections.

Current Limitations of MALDI-IMS and Nano-PALDI-IMS as a Solution

Despite the promising capability of MALDI-IMS, this technique still has several critical limitations. An important challenge is the improvement in spatial resolution toward ion imaging within cellular organelles, which requires resolution at the sub-micrometer level. However, when MALDI is employed as an ionization technique for IMS, the nature of the MALDI process requires the formation of analyte-matrix co-crystals on the tissue section. The typical size of these co-crystals is >50 μm; they function to protect the analyte molecules from direct laser irradiation, i.e., act as a "cushion" and eventually enhance the soft ionization of biomolecules. Unfortunately, this crystal size effectively limits the spatial resolution of IMS to as large as the crystal size. In this regard, imaging with SIMS, a matrix-free ionization technique, has already achieved submicron spatial resolution. In SIMS, the use of a tightly focused ion beam for ionization offers a resolution at several tens of nanometers and has been successfully used to visualize sub-cellular structures in biological samples (Monroe et al. 2005; Ostrowski et al. 2004). However, SIMS is a much "harder" ionization method than MALDI, and consequently, it is not the best choice for intact ionization of various biomolecules because heavier molecules (<1000 Da) and molecules with easily fragmented groups cannot be ionized in their intact from using SIMS (Kraft et al. 2006). In order to overcome these issues, the current authors have reported an NP-assisted laser desorption/ionization (nano-PALDI)-based IMS technique, in which the organic matrix is replaced with NPs, and therefore, the matrix crystallization process is eliminated (Taira et al. 2008). Figure 6 presents a simple illustration of the relationship among MALDI, SIMS, and nano-PALDI.

This novel nano-PALDI-IMS technique affords high-resolution imaging of complex biological specimens (Taira et al. 2008). For this purpose, functional nanoparticles (fNPs) with a diameter of 3.7 ± 0.1 nm were also developed. The inset of Fig. 7 shows the structure of the developed fNPs. Surface-positioned silicon dioxide (SiO_2) groups could be used for attaching various chemical groups, and in the study, hydroxyl

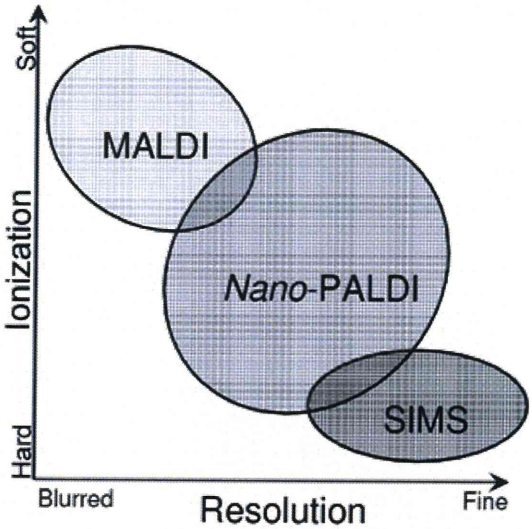

Fig. 6. Applicable areas of matrix-assisted laser desorption/ionization (MALDI), nanoparticle-assisted laser desorption/ionization (nano-PALDI) and secondary ion mass spectrometry (SIMS) techniques in IMS. Three different IMS techniques are compared based on the resolution and the severity of ionization.

and amino groups were linked, resulting in improved ionization efficiency for the small molecules. The improved ionization efficiency presumably results from the capture of analyte molecules close to the fNP surface, which facilitates efficient transfer of laser energy from the NP to the analyte molecules (Fig. 8h). Figure 7 shows representative mass spectra of mouse brain sections obtained using fNP and DHB as respective matrices. Comparison of the spectra shows that in the mass range of $700 < m/z < 900$, signals derived from phospholipids and glycolipids were detected at almost the same intensity using either technique. On the other hand, in the lower mass range, i.e., $100 < m/z < 500$, a larger number of mass peaks with higher intensities were detected using fNP as matrix, whereas when DHB was used as a matrix, most of the intense peaks detected in the same mass region were derived from DHB-originated ions. This example clearly demonstrates the highly effective nature of nano-PALDI for small molecule imaging.

Another important advantage: spraying fNP on the tissue surface did not alter the optical image of the biological tissue surface (Fig. 8). In contrast, when the mouse brain sections were sprayed with a DHB solution, non-homogeneous DHB crystals were formed on the section, which obscured the optical view of the sample surface (Fig. 8a–b). This obscurity resulting

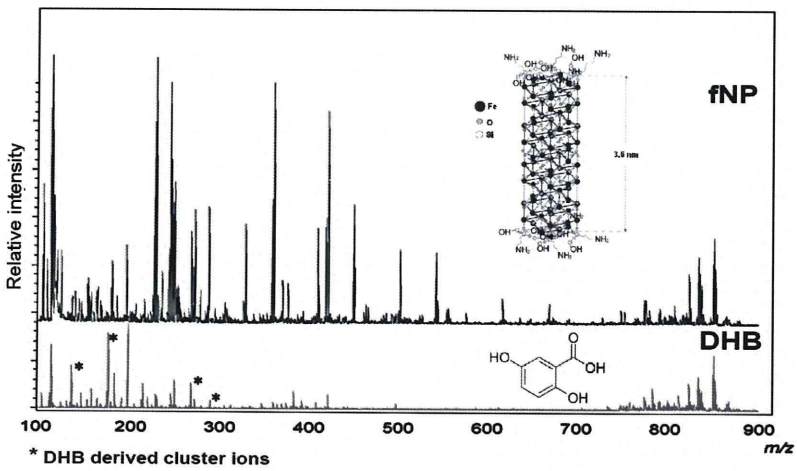

Fig. 7. Representative mass spectra of mouse brain section obtained using functional nanoparticle (fNP) and DHB as respective matrices. Either fNP or 2,5-dihydroxybenzoic acid (DHB) was applied as a matrix on a mouse brain section, and mass spectra were obtained from each applied spot. These mass spectra clearly demonstrate the elimination of DHB-derived background signals as well as increased detection sensitivity for small molecules within the 100 < *m/z* < 600 range using fNP as a matrix. Reprinted from Sahashi et al. 2010 with the permission of Elsevier, Ltd.

from crystal formation with DHB makes it difficult to predefine the tissue region of interest before conducting MS or IMS measurements. Owing to the quite large number of MS measurements performed during the IMS experiment, which is equal to the number of pixels of the resulting image, there is a practical requirement that the measurement area be limited (generally, ten thousand MS measurements per single IMS analysis is the upper limit mainly because of the huge size of the data set). In addition, SEM observation of the DHB coated tissue surface revealed inhomogeneous needle like crystals having typical lengths of > 50 μm (Fig. 8c), which limits the spatial resolution of MALDI-IMS, as described above. In contrast, because of the extremely small particle size of fNPs, spraying these fNPs onto the tissue surface did not alter the optical image of the tissue structure (Fig. 7d–e), thereby allowing the researcher to perform MS and IMS measurements with concomitant optical observation of the tissue structure (using a CCD camera with which MALDI-MS instruments are generally equipped). The SEM images demonstrate that the fNPs which were sprayed onto the tissue surface were distributed in a manner similar to the as-synthesized particles (Fig. 8f–g).

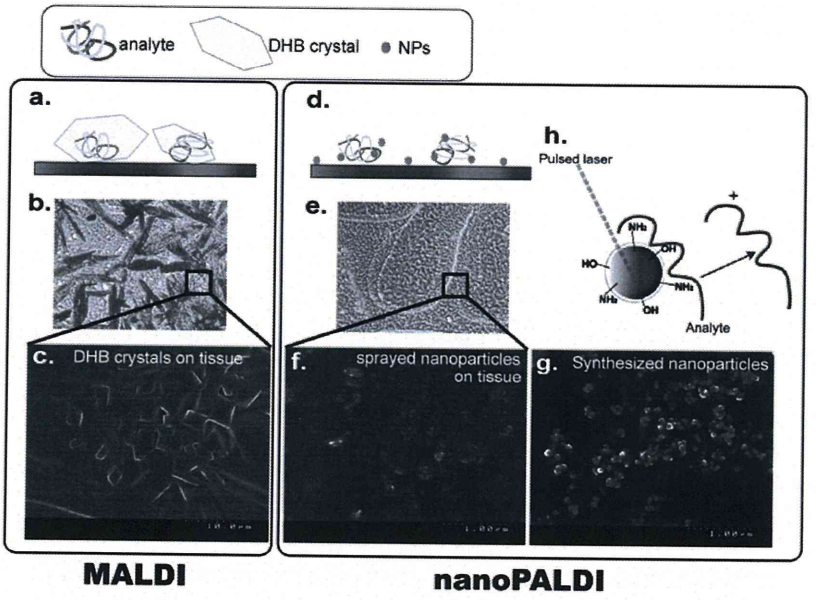

Fig. 8. Principle of nanoparticle-assisted laser desorption/ionization (nano-PALDI) and matrix-assisted laser desorption/ionization based imaging mass spectrometry (MALDI-IMS). Shown are schematic, light microscopic, and scanning electron microscopy images of 2,5-dihydroxybenzoic acid (DHB)/nanoparticles (NPs) applied to biological tissue section. MALDI requires formation of analyte-matrix co-crystals with typical sizes of <50 μm on the tissue section, which limits the spatial resolution of MALDI-IMS (left), whereas in nano-PALDI, the use of NPs as the ionization enhancing reagent eliminates formation of such crystals (right) and enables clear observation of tissue surface even during mass spectrometry measurement. Modified from Taira et al. 2008 with the permission of ACS Publications.

The considerable advantage of nano-PALDI-based IMS in the low *m/z* region is clearly demonstrated in Fig. 9, which shows the results of the feasibility study using IMS measurements performed with both nano-PALDI and MALDI. Tissue samples were obtained from rat cerebella, and NP fluid was sprayed on a thin tissue section of the cerebellum (Fig. 9b, d, f), whereas successive tissue sections were treated by application of DHB (Fig. 9c, e, g). Each IMS measurement was performed at spatial resolution of 15 μm, using a MALDI-TOF/TOF-type instrument. Consistent with the aforementioned features of fNPs, the comparative analysis showed that the use of fNP produced a unique ion distribution image that could not be detected when DHB was used (Fig. 9e and g), and a much finer ion distribution image (Fig. 9d and f), without background noise. On the other hand, ion images with DHB showed crystal-shaped ion localization patterns (especially in Fig. 9g), suggesting that analyte molecules could

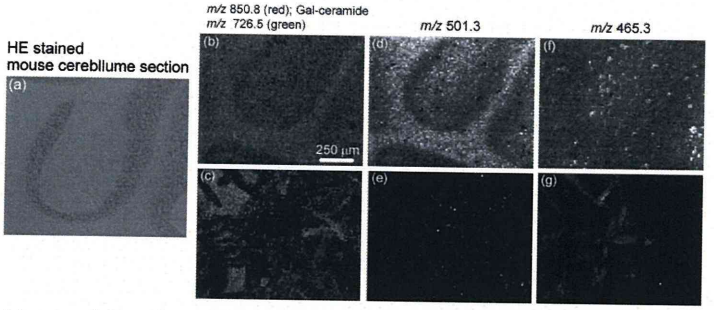

Fig. 9. Nanoparticle-assisted laser desorption/ionization based imaging mass spectrometry (nano-PALDI-IMS) of low molecular weight compounds showing improved ion distribution image quality. Optical images of rat cerebellum tissue before spraying with nanoparticles (NPs) (a) and 2,5-dihydroxybenzoic acid (DHB) solution, and ion images obtained with NPs (b, d, f) and DHB (c, e, g) are shown. Visualized ions were identified as galactosylceramide (C24h:0) and phosphotidylcholine (PC) (diacyl-34:2) by tandem mass spectrometry on both DHB and NP coated sections. Reprinted from Taira et al. 2008 with the permission of ACS Publications.

Color image of this figure appears in the color plate section at the end of the book.

only be ionized from the analyte-matrix co-crystals. Even though the results are only representative, this example clearly demonstrates that the organic matrix crystals severely limit the IMS spatial resolution.

Analysis of Molecular Distribution of Sulfatide

As frequently described, lipids constitute half of the dry weight in the brain, and play important roles especially as fundamental building components of cell structures and as signaling molecules with strong bioactivity (Bosio et al. 1998). Owing to the technical difficulty presented by the insolubility of lipids in aqueous media, the study of lipids has been mainly performed using traditional biochemical techniques. The emergence of IMS as a tool for the imaging of lipids has had significant impact, because there was previously no established technique for two-dimensional mapping of lipids, whereas transcripts can be visualized with oligonucleotide probes using *in situ* hybridization and proteins can be visualized using immunohistochemistry with appropriate antibodies. In this context, lipid imaging by IMS, particularly utilizing nano-PALDI based IMS should prove critical to the interpretation of the role of lipids in brain research.

Nano-PALDI-IMS has also been applied to the mapping of sulfatide distribution. Sulfatides are important lipid components of the myelin sheath. A direct correlation between sulfatide deficiency and neurological disorders, such as Alzheimer's disease (Han et al. 2002) has been reported. Furthermore, one decomposition pathway of sulfatides is catalyzed by

arylsulfatase A (ASA) and the functional deficiency of ASA results in metachromatic leukodystrophy (MLD), which causes the accumulation of sulfatide in lysozymal storage deposits, and eventually, demyelination in the peripheral and central nervous systems (PNS and CNS) (Krivit 2004). In addition, structural variations of sulfatide arise from hydroxylation of the fatty acid moiety as shown by the arrow in Fig. 10. The hydroxylation is catalyzed by fatty acid 2-hydroxylase (FA2H), which also causes leukodystrophy with spastic paraparesis and dystonia (Kruer et al. 2010).

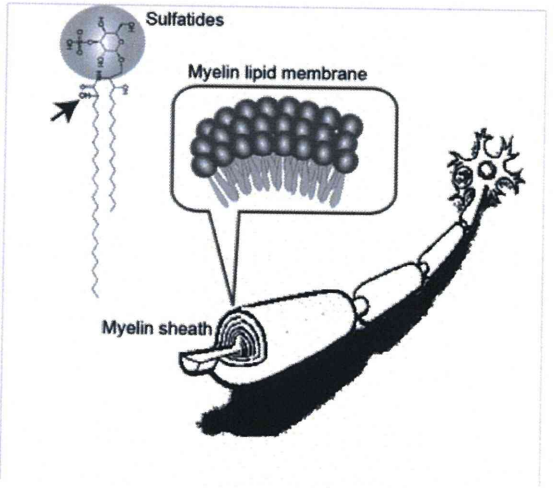

Fig. 10. Schematic representation of myelin sheath and one of its major lipid components, sulfatides. Nanoparticle-assisted laser desorption/ionization imaging mass spectrometry (nano-PALDI-IMS) was applied to the mapping of sulfatide distribution. Sulfatides are important lipid components of the myelin sheath. The black arrow indicates the hydroxylation site on the fatty acid moiety that causes structural variation.

The distribution pattern of sulfatide in the brain has been assessed by using the anti-sulfatide antibody to track the distribution of sulfatide in the CNS and PNS of rodent brains (Pernber et al. 2002). However, immunostaining with this antibody did not allow for discrimination of the fatty acid moiety of this lipid specie or of the presence/absence of the abovementioned hydroxylation. In comparison, based on the MS detection principle, distinct images of these species were obtained using IMS (Ageta et al. 2009). Figure 11 shows different regions of the dentate gyrus of rat hippocampus, such as the granular cell layer (GCL), inner molecular layer (IML), and middle molecular layer (MML) (left column), as well as the intensity of the different mass peaks in these regions (right column). It was found that the intensity of the peaks with *m/z* of 906.3,

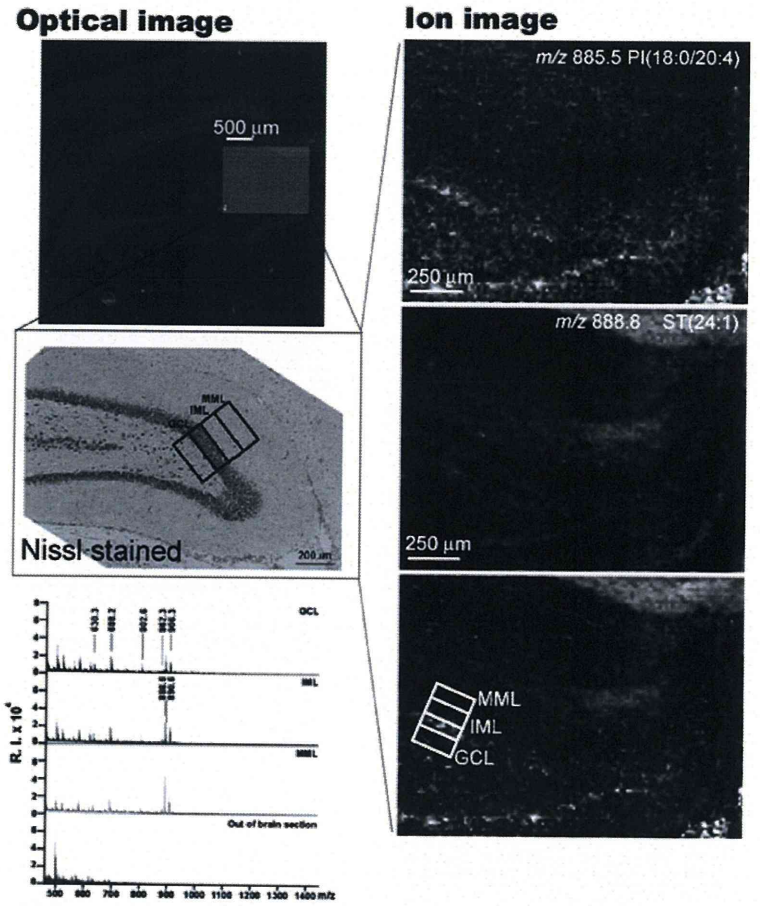

Fig. 11. Nanoparticle-assisted laser desorption/ionization improves spatial resolution in imaging mass spectrometry (IMS). Optical image of rat hippocampus indicating measurement area for nanoparticle-based IMS is shown along with Nissl-stained section indicating fine layer structure of rat hippocampus (left panels). Ion images, which reveal hippocampal layer specific distribution of phosphatidylinositol (18:0/20:4) at *m/z* 885.5 and sulfatide (24:1) at *m/z* 888.8, are presented (right panels). GCL = granular cell layer, IML = inner molecular layers, and MML = middle molecular layers. Reprinted from Ageta et al. 2009 (left column) and Sugiura and Setou 2010b (right column) with the permission of Springer.

Color image of this figure appears in the color plate section at the end of the book.

904.6, 890.6, and 888.6 was higher in the MML region than in the GCL and IML regions, whereas the mass peaks with *m/z* of 862.3, 802.6, 688.2, and 630.3 were detected in the GCL, IML, and MML regions only, indicating their biological origin. Therefore, this technique can potentially be used to explore physiological processes for better understanding of diagnostics and the pathology of neurological disorders, such as leukodystrophy and Alzheimer's disease (Ageta et al. 2009).

Key Facts

- A key fact about MALDI-imaging mass spectrometry (IMS) is that it is an MS-based molecular imaging technique with the following unique advantages. (1) MALDI-IMS can be used for the visualization of the distribution of large numbers of biomolecules in cells and tissues, ranging from small metabolite molecules to much larger proteins. (2) MALDI-IMS does not require any specific chemical labels or probes. (3) MALDI-IMS is a "non-targeted" imaging method. (4) MALDI-IMS enables the simultaneous imaging of multiple types of molecular species.
- A key fact about nanoparticle (NP)-assisted laser desorption/ionization (nano-PALDI)-based IMS is that it is an IMS technique, in which the organic matrix is replaced with NPs such as gold, silver, and titanium. Recently, researchers have begun using NPs for MS research owing to the progress in the development of NP technology, which has made various kinds of NPs available. In MS research, the use of NPs has been studied particularly in the analyses of small molecules, because of the following advantages. (1) The use of nano-PALDI may eliminate background noise generated by organic matrix compounds. (2) Judicious choice of NPs allows for the efficient analysis of analyte molecules that are otherwise difficult to ionize using conventional organic matrices.

Summary

- Imaging mass spectrometry (IMS) enables visualization of the distribution of various biomolecules in biological tissue sections.
- IMS has several unique advantages—(1) It does not require any specific chemical labels or probes. (2) It is a "non-targeted" imaging method. (3) The simultaneous imaging of multiple types of molecular species is available.
- MALDI-IMS in particular, which is a soft ionization method using an organic "matrix," can be used for a large number of biomolecules ranging from small metabolite molecules to much larger proteins.

- Although MALDI-based IMS has promising capacity for the imaging of small metabolites, this technique has a critical problem in spatial resolution derived from matrix crystallization.
- In nanoparticle (NP)-assisted laser desorption/ionization (nano-PALDI)-based IMS, the organic matrix is replaced with NPs, and therefore, the matrix crystallization process is eliminated; therefore, it can be used to overcome the resolution problems of MALDI-IMS.
- Recent development of NPs with different core metals, surface modifications, and particle diameters has expanded the measurable range of analytes as well as the application of the analyses to physiological processes and the diagnosis and pathophysiology of complex biological process, especially in the brain.

Abbreviations

ASA	:	Arylsulfatase A
AuNP	:	Gold Nanoparticle
AgNP	:	Silver Nanoparticle
CCD	:	Charge-Coupled Device
CHCA	:	α-Cyano-4-Hydroxycinnamic Acid
CNS	:	Central Nervous System
DHB	:	Dihydroxy Benzoic Acid
DNA	:	Deoxyribonucleic Acid
ESI	:	Electrospray Ionization
FA2H	:	Fatty Acid 2-Hydroxylase
fNP	:	Functional Nanoparticle
GCL	:	Granular Cell Layer
HE	:	Hematoxilin-Eosin
IML	:	Inner Molecular Layer
IMS	:	Imaging Mass Spectrometry
ITO	:	Indium Tin Oxide
MALDI	:	Matrix-Assisted Laser Desorption/Ionization
MLD	:	Metachromatic Leukodystrophy
MML	:	Middle Molecular Layer
MS	:	Mass Spectrometry
m/z	:	Mass-to-Charge Ratio
nano-PALDI	:	Nanoparticle-Assisted Laser Desorption/Ionization
NP	:	Nanoparticle
NSCLC	:	Non-Small Cell Lung Cancer
PC	:	Phosphotidylcholine
PNS	:	Peripheral Nervous System
SEM	:	Scanning Electron Microscopy
SIMS	:	Secondary Ion Mass Spectrometry

SiO_2	:	Silicon dioxide
siRNA	:	Short-Interfering Ribonucleic Acid
TiO_2	:	Titanium Dioxide
TOF	:	Time-of-Flight
WBA	:	Whole-Body Autoradiography

Key Terms

- MS (Mass spectrometry): Analytical technique that measures the mass (m)-to-charge (z) ratio of charged atoms, molecules, and molecular clusters/fragments.
- IMS (Imaging MS): Molecular imaging technique based on MS.
- MALDI (Matrix-assisted laser desorption/ionization): A soft ionization method used for MS using an analyte ionization-enhancing reagent, called a matrix, which allows the analysis of biomolecules and large organic molecules.
- NP (nanoparticle): A particle whose diameter is 100~1000 nm.
- nano-PALDI (NP-assisted laser desorption/ionization): An ionization method used for MS using NP as an analyte ionization-enhancing reagent.

References

Ageta, H., S. Asai, Y. Sugiura, N. Goto-Inoue, N. Zaima and M. Setou. 2009. Layer-specific sulfatide localization in rat hippocampus middle molecular layer is revealed by nanoparticle-assisted laser desorption/ionization imaging mass spectrometry. Med. Mol. Morphol. 42: 16–23.

Bosio, A., E. Binczek, W.F. Haupt and W. Stoffel. 1998. Composition and biophysical properties of myelin lipid define the neurological defects in galactocerebroside- and sulfatide-deficient mice. J. Neurochem. 70: 308–315.

Chaurand, P., J.L. Norris, D.S. Cornett, J.A. Mobley and R.M. Caprioli. 2006. New developments in profiling and imaging of proteins from tissue sections by MALDI mass spectrometry. J. Proteome Res. 5: 2889–2900.

Chaurand, P., S.A. Schwartz and R.M. Caprioli. 2004. Profiling and Imaging Proteins in Tissue Sections by MS. Anal. Chem. 76: 86–93.

Chen, W.Y. and Y.C. Chen. 2006. Affinity-based mass spectrometry using magnetic iron oxide particles as the matrix and concentrating probes for SALDI MS analysis of peptides and proteins. Anal. Bioanal. Chem. 386: 699–704.

Chiu, T.C., L.C. Chang, C.K. Chiang and H.T. Chang. 2008. Determining estrogens using surface-assisted laser desorption/ionization mass spectrometry with silver nanoparticles as the matrix. J. Am. Soc. Mass. Spectrom. 19: 1343–1346.

Han, X., D, M.H., D.W. McKeel Jr., J. Kelley and J.C. Morris. 2002. Substantial sulfatide deficiency and ceramide elevation in very early Alzheimer's disease: potential role in disease pathogenesis. J. Neurochem. 82: 809–818.

Karas, M. and F. Hillenkamp. 1988. Laser desorption ionization of proteins with molecular masses exceeding 10,000 daltons. Anal. Chem. 60: 2299–2301.

Khatib-Shahidi, S., M. Andersson, J.L. Herman, T.A. Gillespie and R.M. Caprioli. 2006. Direct molecular analysis of whole-body animal tissue sections by imaging MALDI mass spectrometry. Anal. Chem. 78: 6448–6456.

Kraft, M.L., P.K. Weber, M.L. Longo, I.D. Hutcheon and S.G. Boxer. 2006. Phase separation of lipid membranes analyzed with high-resolution secondary ion mass spectrometry. Science 313: 1948–1951.

Krivit, W. 2004. Allogeneic stem cell transplantation for the treatment of lysosomal and peroxisomal metabolic diseases. Springer Semin. Immunopathol. 26: 119–132.

Kruer, M.C., C. Paisan-Ruiz, N. Boddaert, M.Y. Yoon, H. Hama, A. Gregory, A. Malandrini, R.L. Woltjer, A. Munnich, S. Gobin, et al. 2010. Defective FA2H leads to a novel form of neurodegeneration with brain iron accumulation (NBIA). Ann. Neurol. 68: 611–618.

Monroe, E.B., J.C. Jurchen, J. Lee, S.S. Rubakhin and J.V. Sweedler. 2005. Vitamin E imaging and localization in the neuronal membrane. J. Am. Chem. Soc. 127: 12152–12153.

Ostrowski, S.G., C.T. Van Bell, N. Winograd and A.G. Ewing. 2004. Mass spectrometric imaging of highly curved membranes during Tetrahymena mating. Science 305: 71–73.

Pernber, Z., M. Molander-Melin, C.H. Berthold, E. Hansson and P. Fredman. 2002. Expression of the myelin and oligodendrocyte progenitor marker sulfatide in neurons and astrocytes of adult rat brain. J. Neurosci. Res. 69: 86–93.

Sahashi, Y., I. Osaka and S. Taira. 2010. Nutrition analysis by nanoparticle-assisted laser desorption/ionisation mass spectrometry. Food Chem. 123: 865–871.

Sherrod, S.D., A.J. Diaz, W.K. Russell, P.S. Cremer and D.H. Russell. 2008. Silver nanoparticles as selective ionization probes for analysis of olefins by mass spectrometry. Anal. Chem. 80: 6796–6799.

Shrivas, K. and H.F. Wu. 2008. Applications of silver nanoparticles capped with different functional groups as the matrix and affinity probes in surface-assisted laser desorption/ionization time-of-flight and atmospheric pressure matrix-assisted laser desorption/ionization ion trap mass spectrometry for rapid analysis of sulfur drugs and biothiols in human urine. Rapid Commun. Mass Spectrom. 22: 2863–2872.

Stoeckli, M., P. Chaurand, D.E. Hallahan and R.M. Caprioli. 2001. Imaging mass spectrometry: a new technology for the analysis of protein expression in mammalian tissues. Nat. Med. 7: 493–496.

Su, C.L. and W.L. Tseng. 2007. Gold nanoparticles as assisted matrix for determining neutral small carbohydrates through laser desorption/ionization time-of-flight mass spectrometry. Anal. Chem. 79: 1626–1633.

Sugiura, Y. and M. Setou. 2010a. Imaging mass spectrometry for visualization of drug and endogenous metabolite distribution: toward in situ pharmacometabolomes. J Neuroimmune Pharmacol. 5: 31–43.

Sugiura, Y. and M. Setou. 2010b. Matrix-Assisted Laser Desorption/Ionization and Nanoparticle-Based Imaging Mass Spectrometry for Small Metabolites: A Practical Protocol. pp. 173–195. *In:* S.S.S. Rubakhin and J.V.V. Sweedler. [eds.] Mass Spectrometry Imaging: Principles and Protocols, Methods Mol. Biol. 656. Springer. New York.

Sunner, J., E. Dratz and Y.C. Chen. 1995. Graphite surface-assisted laser desorption/ ionization time-of-flight mass spectrometry of peptides and proteins from liquid solutions. Anal. Chem. 67: 4335–4342.

Taira, S., S. Moritake, T. Hatanaka, Y. Ichyanagi and M. Setou. 2009. Functionalized Magnetic Nanoparticles as an *In Vivo* Delivery System pp. 571–587. *In:* J.W. Lee and R.S. Foote. [eds.] Micro and Nano Technologies in Bioanalysis: Methods and Protocols, Methods Mol. Biol. 544. Humana press. New York.

Taira, S., Y. Sugiura, S. Moritake, S. Shimma, Y. Ichiyanagi and M. Setou. 2008. Nanoparticle-assisted laser desorption/ionization based mass imaging with cellular resolution. Anal. Chem. 80: 4761–4766.

Tanaka, K., H. Waki, Y. Ido, S. Akita, Y. Yoshida, T. Yoshida and T. Matsuo. 1988. Protein and polymer analyses up to *m/z* 100 000 by laser ionization time-of-flight mass spectrometry. Rapid Commun. Mass Spectrom. 2: 151–153.

Watanabe, T., K. Okumura, H. Kawasaki and R. Arakawa. 2009. Effect of urea surface modification and photocatalytic cleaning on surface-assisted laser desorption ionization mass spectrometry with amorphous TiO_2 nanoparticles. J. Mass Spectrom. 44: 1443–1451.

Wu, H.P., C.J. Yu, C.Y. Lin, Y.H. Lin and W.L. Tseng. 2009. Gold nanoparticles as assisted matrices for the detection of biomolecules in a high-salt solution through laser desorption/ionization mass spectrometry. J. Am. Soc. Mass. Spectrom. 20: 875–882.

Yanagisawa, K., Y. Shyr, B.J. Xu, P.P. Massion, P.H. Larsen, B.C. White, J.R. Roberts, M. Edgerton, A. Gonzalez and S. Nadaf. 2003. Proteomic patterns of tumour subsets in non-small-cell lung cancer. Lancet 362: 433–439.

Yang, H.J., I. Ishizaki, N. Sanada, N. Zaima, Y. Sugiura, I. Yao, K. Ikegami and M. Setou. 2010. Detection of characteristic distributions of phospholipid head groups and fatty acids on neurite surface by time-of-flight secondary ion mass spectrometry. Med. Mol. Morphol. 43: 158–164.